Appendix I

Radiocarbon dating

Peter Marshall, Alex Bayliss, John Meadows, Christopher Bronk Ramsey, Gordon Cook & Hans van der Plicht

The use of the radiocarbon method in conjunction with palaeo-environmental reconstruction using palynology and plant macrofossils has a lengthy pedigree (e.g. Smith & Pilcher, 1973; Birks & Birks, 1980; Lowe & Walker, 1997; see Chapter 3). Fifty-seven radiocarbon age determinations have been obtained from twelve sites that were investigated as part of the Swale-Ure Project. These are presented, in the context of the sites dated, in Chapter 3 of the monograph. This appendix was submitted as a stand-alone contribution, giving information about methods used and interpretation of the dates.

Methods

Twenty-eight samples were processed at the Oxford Radiocarbon Accelerator Unit at the University of Oxford by Accelerator Mass Spectrometry (AMS) in 2003 and 2004, according to procedures described by Bronk Ramsey and Hedges (1997) and Bronk Ramsey *et al*. (2000, 2004). A further fifteen samples were processed and measured by Accelerator Mass Spectrometry (AMS) at the Centre for Isotope Research, Groningen University, The Netherlands, in 2004, following the procedures described by Aerts-Bijma *et al*. (1997, 2001) and van der Plicht *et al*. (2000). The final fourteen samples were processed at the Scottish Universities Research and Reactor Centre in East Kilbride between 2004 and 2006. Thirteen of these (denoted by the laboratory prefix SUERC-) were measured by AMS at the Scottish Universities Environmental Research Centre AMS Facility. Details of the sample preparation have been provided by Slota *et al*. (1987) and measurement was described by Xu *et al*. (2004). One sample (laboratory prefix GU-) was prepared using the methods outlined by Stenhouse and Baxter (1983) and measured using liquid scintillation spectrometry (Noakes *et al*., 1965). All three laboratories maintain continual programmes of quality assurance procedures, in addition to participation in international inter-comparisons (Scott, 2003). These tests indicate no laboratory offsets and demonstrate the validity of the precision quoted.

In addition to these samples, submitted as part of the ALSF-funded project, a further eight samples had been dated previously as part of studies in the Swale-Ure project area (Howard *et al*., 2000; Tipping, 2000). These samples were dated at Beta Analytic Inc by AMS using methods outlined at http://www.radiocarbon.com/.

Results and Calibration

Having already been presented in stratigraphical context in Chapter 3, the radiocarbon results are provided in Tables 1–15 (at the end of this document), in which they are quoted in accordance with the international standard known as the Trondheim convention (Stuiver & Kra, 1986). They are conventional radiocarbon ages (Stuiver & Polach, 1977). The calibrations of the results, relating the radiocarbon measurements directly to calendar dates, are given in Tables 1–15 and in Figures 1–15. All have been calculated using the calibration curve of Reimer *et al*. (2004) and the computer program OxCal (v3.10) (Bronk Ramsey, 1995, 1998, 2001). The calibrated date ranges cited in the text are those for 95% confidence. They are quoted in the form recommended by Mook (1986), with the end points rounded outwards to 10 years if the error term is greater than or equal to 25 radiocarbon years. The ranges quoted in italics are *posterior density estimates* derived from mathematical modelling (see below). The ranges in plain type have been calculated according to the maximum intercept method (Stuiver & Reimer, 1986). All other ranges are derived from the probability method (Stuiver & Reimer, 1993).

Bayesian modelling

A Bayesian approach (Buck *et al*., 1996; Blockley *et al*., 2004) has been adopted for the interpretation of the results from two sites: Nosterfield F45 and Sharow Mires (see Chapter 3.2.1 and 3.5). Although the simple calibrated dates are accurate estimates of the ages of the samples, this is not usually the priority; it is the dates of the events (e.g. the start of peat growth) represented by the samples that are of interest. The dates of such events can be estimated not only using the absolute dating information from the radiocarbon measurements on the samples, but also by using the stratigraphical relations between samples.

Fortunately, methodology is now available that allows the combination of these different types of information explicitly, to produce realistic estimates of the dates of interest. It should be emphasised that the posterior density estimates produced by this modelling are not absolute; they are interpretative estimates, which can and will change as further data become available and as other researchers choose to model the existing data from different perspectives.

The technique used is a form of Markov Chain Monte Carlo sampling; it has been applied using the program OxCal v3.10 (http://www.rlaha.ox.ac.uk/), which uses a mixture of the Metropolis-Hastings algorithm and the more specific Gibbs sampler (Gilks *et al*., 1996; Gelfand & Smith, 1990). Details of the algorithms employed by this program are available from the on-line manual or from Bronk Ramsey (1995, 1998, 2001). The algorithm used in the models described below can be derived from the structures shown in Figures 1b and 15.

Sample selection

Potential samples for radiocarbon measurement came from two environmental contexts, Holocene and Lateglacial limnic/peat sediments and Holocene fluvial sequences (see Chapter 3). The first group of sediments were mainly deposited in meltwater channels, kettle holes or gypsum collapse features**,** as well as abandoned fluvial channels (e.g. Marfield – Chapter 3.4); the second group of contexts comprised organic muds and peats with variable quantities of gravels and sands deposited on floodplains and in oxbow lakes and other sections of abandoned river channel. Both these contexts pose challenges in terms of identifying suitable samples for radiocarbon analysis, as understanding the taphonomy of samples is key to their reliability in providing accurate chronologies.

Since the early 1990s there has been a tendency for radiocarbon measurements on samples from Lateglacial and early Holocene contexts to be obtained by AMS, using plant macrofossil material. Two main factors have influenced this:

- **sample size** – reduction in the size of sample required (0.2 mg of organic carbon), thus increasing the degree of stratigraphical resolution.
- **taphonomy** – the belief that plant macrofossils are more reliable than bulk samples of sediment matrix, as the source of carbon in the former is known and they are not made up of heterogeneous material that could be of different ages (Lowe &Walker, 2000; Walker *et al*., 2001).

Lateglacial and early Holocene contexts

In order of preference, the following samples for radiocarbon analysis were identified from Lateglacial and early Holocene contexts:

1. **Terrestrial macrofossils**. Preferably 'fragile' remains that are unlikely to have survived reworking. They should be short-lived plants, identifiable to species; for wood, specimens should have bark or represent the outer rings of a tree.

   Aquatic macrofossils (e.g. *Potamogeton*) were avoided because such plants may utilize dissolved CO_2, resulting in the uptake of 'old' carbon (Bowman, 1990). In addition, moss species such as *Scorpidium scorpioides* were also preferentially avoided, given the possibility that at least some of the carbon fixed by them during photosynthesis could be of 'old' carbon (M. Proctor, pers comm.).

2. **Bulk organic sediment samples**. Bulk radiometric measurements were made on the humin (acid washed, alkali insoluble) fraction, as the humic (acid washed alkali soluble) fraction may be mobile due to its solubility in alkaline environments, especially sodium-based gypsum.

   Due to the nature of the sampling sites (most sediments were sampled with corers), the retrieval of enough sediment for 'bulk' radiometric measurement (>250g) was in most cases impractical. Moreover, AMS measurement of 'bulk' samples was avoided because of the potential of inhomogeneity problems (a small amount of contaminant will have a greater effect because of the size of sample (Shore *et al*., 1995).

Holocene contexts

The later Holocene sequences comprised, for the most part, organic muds and peats deposited in flood plain and ox-bow contexts, containing variable quantities of plant macrofossils ranging in size from seeds to trees. In order of preference the following types of samples were identified:

1 **Terrestrial macrofossils (I)** as above, from organic mud and peat deposits

2 **Terrestrial macrofossils (II)** from gravels and sands. However, these were felt to be less reliable than (1) due to the possibilities of reworking.

3 **Bulk organic sediment samples** – as above

Objectives of the dating programme

The overall objective of the radiocarbon dating programme was to contribute to the assessment of the fluvial and landscape evolution of the Swale-Ure Washlands since deglaciation and to understanding of the timing and impact of human activity during this period. In order to achieve this overall objective, investigations at individual study sites also required the dating programme to contribute to more site-specific objectives, which are referred to in the following sections that discuss the results from the various sites (see also the various sections of Chapter 3).

Nosterfield, F45 and associated cores (Tables 1–4; Figs 1–4)

Nine samples were submitted from a possible gypsum solution feature (Chapter 3.2.1), formed in the Nosterfield fan gravels, that had accumulated 281 cm of organic sediments, providing a valuable record of local prehistoric vegetational change close to the

Table1: Details of radiocarbon dates from Nosterfield, F45

Laboratory code	Sample depth	Material	$\delta^{13}C$ (‰)	Radiocarbon age BP	Weighted mean	Calibrated date range (95% confidence)	*Posterior Density Estimate (95% probability)*
Beta-143452	0–1cm	Peat	-29.0	2330±40		480–360 cal. BC	-
OxA-13558	22–23cm	Plant macrofossils: *Eleocharis* sp. nutlets; *Carex* sp. nutlets; *Ranunculus flammula achenes*	-26.3	2256±32		400–200 cal. BC	*380–350 (5%) or 320–200 (90%) cal. BC*
OxA-13559	23–24cm	Plant macrofossils: *Eleocharis* sp. nutlets; *Carex* sp. nutlets; *Ranunculus flammula achenes*; *Potentilla* sp. *achenes*	-26.7	2229±34		390–190 cal. BC	*390–240 cal. BC*
GrA-25299	33–34cm	Plant macrofossil: unidentified bark	-30.2	2365±35		520–380 cal. BC	*510–380 cal. BC*
GrA-25300	41–42cm	Plant macrofossil: unidentified bark	-30.8	2395±35		740–390 cal. BC	*750–640 (18%) or 550–390 (77%) cal. BC*
GrA-25301	93–94cm	Plant macrofossil: unidentified bark	-27.4	4050±40	T'=2.2; ν=1; T'(5%)=3.8	2840–2470 cal. BC	*2830–2810 (2%) or 2700–2470 (93%) cal. BC*
OxA-13494	93–94cm	Plant macrofossil: unidentified bark	-26.8	4124±30		2880–2570 cal. BC	*2860–2800 (8%) or 2780–2570 (87%) cal. BC*
OxA-13553	119–120cm	Wood, possibly *Alnus glutinosa*	-27.1	4193±31		2900–2620 cal. BC	*2900–2620 cal. BC*
OxA-13530	128–129cm	Plant macrofossil: charred twig	-25.0	11,675±50		11,740–11,430 cal. BC	-
GrA-25355	145cm	Plant macrofossil: *Alnus*	-27.1	4000±50		2830–2350 cal. BC	-
Beta-143456	280–281cm	Organic silt	-26.2	10,180±60		10,140–9,660 cal. BC	-

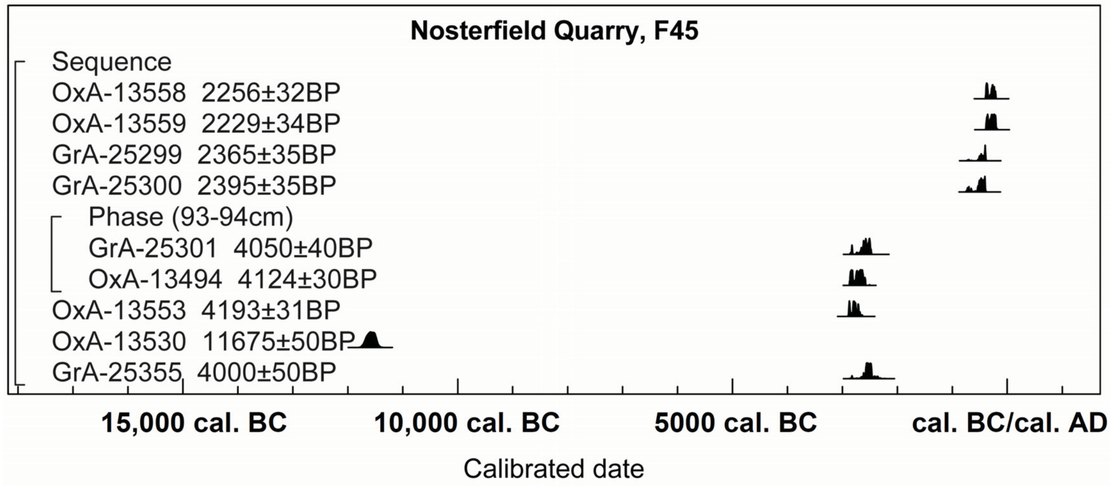

Figure 1a: Probability distributions of dates from Nosterfield F45. Each distribution represents the relative probability that an event occurred at a particular time. These distributions are the result of simple radiocarbon calibration (Stuiver & Reimer, 1993).

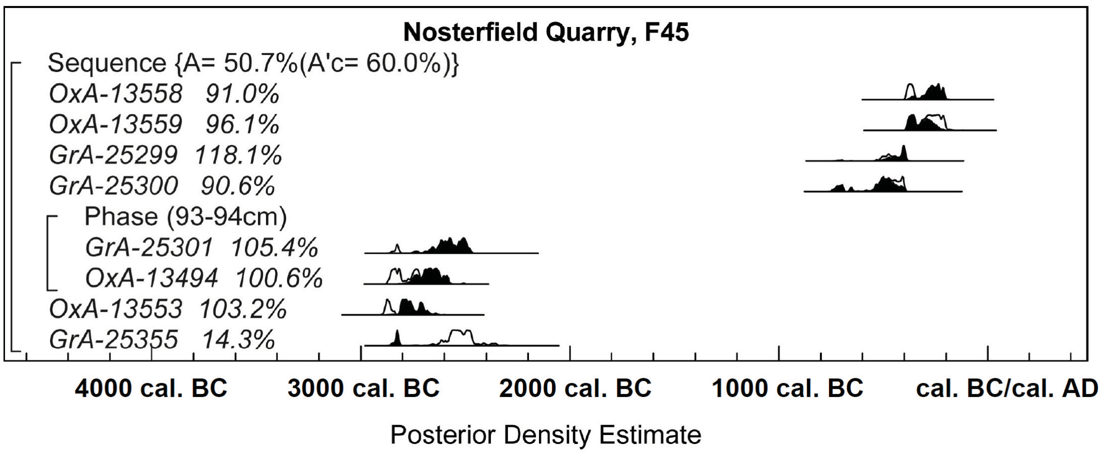

Figure 1b: Probability distributions of dates from Nosterfield F45: each distribution represents the relative probability that an event occurs at a particular time. For each of the radiocarbon dates two distributions have been plotted, one in outline, which is the result of simple radiocarbon calibration, and a solid one, which is based on the chronological model used. The large square brackets down the left hand side along with the OxCal keywords define the model exactly.

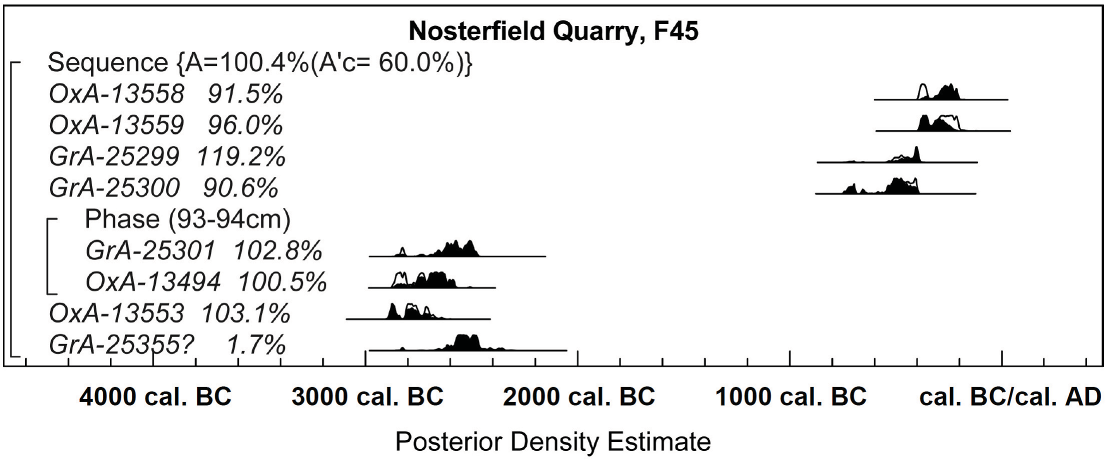

Figure 1c: Probability distributions of dates from Nosterfield F45: each distribution represents the relative probability that an event occurs at a particular time. For each of the radiocarbon dates two distributions have been plotted, one in outline, which is the result of simple radiocarbon calibration, and a solid one, which is based on the chronological model used. A question mark (*?*) indicates that the result has been excluded from the model. The large square brackets down the left hand side along with the OxCal keywords define the model exactly.

Table 2: Details of radiocarbon dates from Nosterfield, F44

Laboratory code	Sample depth	Material	δ13C (‰)	Radiocarbon age BP	Calibrated date range (95% confidence)
Beta-143453	0–1cm	Peat	-28.2	3110±30	1440–1310 cal. BC
Beta-143455	239–240cm	Peat	-26.2	11,140±60	11,240–10,960 cal. BC

Table 3: Details of radiocarbon dates from Nosterfield, F46

Laboratory code	Sample depth	Material	δ13C (‰)	Radiocarbon age BP	Calibrated date range (95% confidence)
Beta-143454	8–9cm	Peat	-28.1	3930±40	2570–2290 cal. BC
Beta-143457	219–220cm	Peat	-28.1	8900±50	8250–7820 cal. BC

Table 4: Details of the radiocarbon date from Nosterfield, Find 14

Laboratory code	Sample depth	Material	δ13C (‰)	Radiocarbon age BP	Calibrated date range (95% confidence)
Beta-143458	9–10cm	Peat	-28.4	9380±50	8790–8490 cal. BC

Thornborough henge complex. In addition, samples from the top and bottom of the organic sequence had been dated previously (Tipping, 2000). These were AMS measurements made on bulk samples; given the problems outlined above with regard to the accuracy of AMS-sized bulk measurements, these earlier data have been excluded from the analysis described below.

The results, shown in Figure 1a, show poor agreement between the stratigraphical position and radiocarbon ages of samples at the base of the core. OxA-13530 (a charred twig) comes from a horizon that shows a decline in *Betula* frequencies and the first record of cereal-type pollen in the vegetation record. The Lateglacial date (11,740–11,430 cal. BC) is thus clearly too old, suggesting that the charred twig might be reworked.

If OxA-1350 is excluded from the analysis (see Fig. 1b), the remaining measurements still show poor agreement between the radiocarbon results and stratigraphy ($A_{overall}$=50.7%), with GrA-25355 seeming to be too young for its stratigraphical position (A=14.4%). An agreement index of >60% has been recommended as the rejection threshold for individual dates, as well as for a series of dates ($A_{overall}$) in which the individual index of agreements for all radiocarbon measurements are combined (Bronk Ramsey, 1995). If GrA-25355 is excluded from the analysis (Fig. 1c) the model shows good overall agreement ($A_{overall}$=100.4%) and provides a robust chronological sequence from the Neolithic to late Iron Age.

A number of other organic sequences from Nosterfield Quarry have been dated previously (Tipping, 2000; Tables 2–4; Figs 2–4); however, given that these were all bulk AMS samples, caution should be exercised in their interpretation (see above).

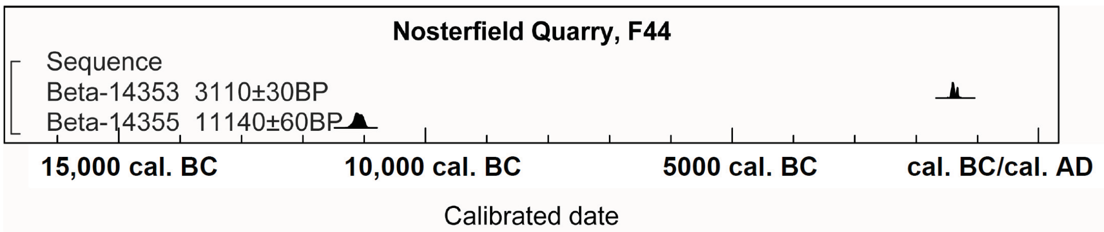

Figure 2: Probability distributions of dates from Nosterfield Quarry, Core F44. Each distribution represents the relative probability that an event occurred at a particular time. These distributions are the result of simple radiocarbon calibration (Stuiver & Reimer, 1993).

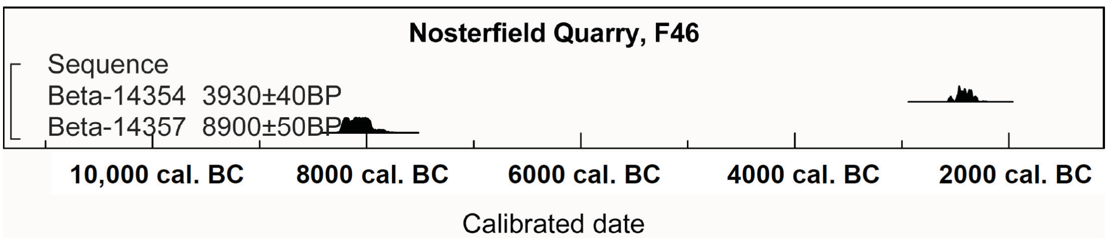

Figure 3: Probability distributions of dates from Nosterfield Quarry, Core F46. Each distribution represents the relative probability that an event occurred at a particular time. These distributions are the result of simple radiocarbon calibration (Stuiver & Reimer, 1993).

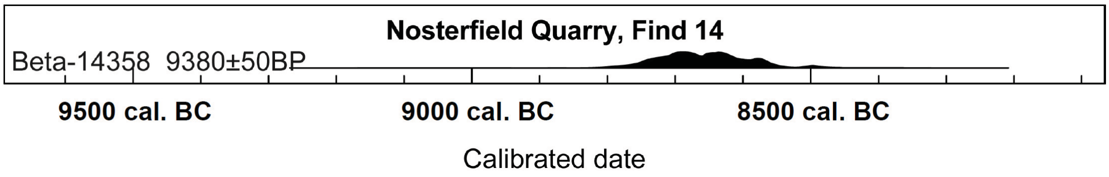

Figure 4: Probability distributions of dates from Nosterfield Quarry, Find 14 (see Tipping, 2000). Each distribution represents the relative probability that an event occurred at a particular time. These distributions are the result of simple radiocarbon calibration (Stuiver & Reimer, 1993).

Nosterfield, Shakehole SH1 (Table 5; Fig. 5)

Five samples were submitted from the site known as 'the Flasks', located in the northern part of the Tarmac quarry at Nosterfield (Chapter 3.2.2). The samples came from a 5 m deep peat sequence that had filled the shake-hole following its formation as a result of dissolution from the underlying Magnesian limestone. The samples were selected with the aim of:

- establishing a chronology for the accumulation of the peat sediments;
- establishing the date of human impact on the landscape as recorded in the palaeoenvironmental record.

The basal measurement OxA-13012 (7705±39 BP) provides a date (6640–6460 cal. BC) for the start of peat inception within the shake-hole and is in agreement with the pollen data, which suggest a mid-Holocene, pre-elm decline, deciduous forest landscape. The two samples from 119–120 cm were selected to date a peak in the pollen record of cereal-type, together with weeds of cultivation (e.g. *Plantago lanceolata*, *Taraxacum* spp. The two measurements GrA-25048 (3230± 40 BP) and OxA-13225 (3427±35 BP) are not statistically consistent (T'=13.7; ν=1; T'(5%)=3.8; Ward & Wilson, 1978). This is potentially the result of selecting specimens for dating from within a 1 cm slice of peat, accumulation of which would not have been an instantaneous event; thus both dates can be regarded as accurate and together they suggest an increased phase of agricultural activity in the mid–late 2nd Millennium cal. BC. Sample GrA-24566 (84–85 cm) provides a date of 980–800 cal. BC (2715±45 BP) for a major landscape change, recorded in the pollen record, from an at least partly wooded local landscape to one completely dominated by non-tree taxa.

Table 5: Details of radiocarbon dates from Nosterfield, SH1

Laboratory code	Sample depth	Material	δ13C (‰)	Radiocarbon age BP	Weighted mean	Calibrated date range (95% confidence)
GrA-24566	84–85cm	Indeterminate bark	-30.0	2715±45		980–800 cal. BC
GrA-25048	119–120cm	Wood: *Alnus* twig	-30.1	3230±40	T'=13.7; ν=1; T'(5%)=3.8	1610–1420 cal. BC
OxA-13225	119–120cm	Plant macrofossils: *Ranunculus* achene, wood and bark, *Carex* sp. nutlet, *Rubus idaeus* fruitstone	-27.5	3427±35		1880–1630 cal. BC
OxA-13104	338–340cm	Plant macrofossils: *Menyanthes trifoliata* seeds, 14 *Betula* fruits, *Carex* twig and nutlet	-24.4	7435±39		6420–6220 cal. BC
OxA-13012	495–496cm	Plant macrofossil: monocot culm (stem)	-25.4	7705±39		6640–6460 cal. BC

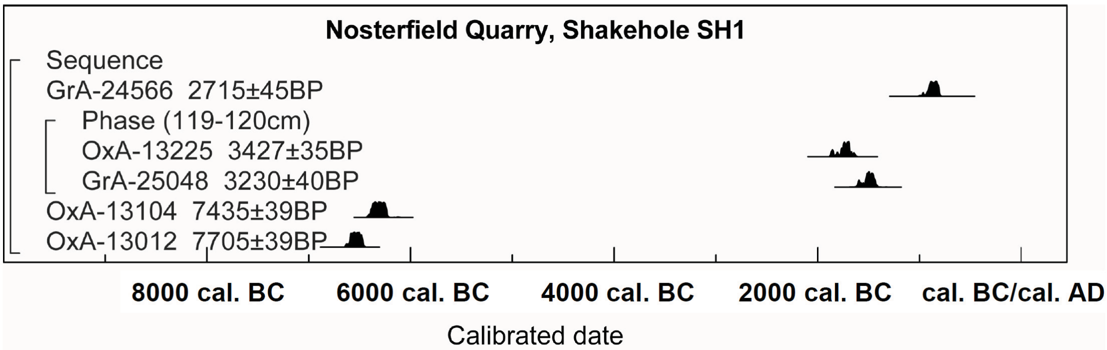

Figure 5: Probability distributions of dates from Nosterfield SH1. Each distribution represents the relative probability that an event occurred at a particular time. These distributions are the result of simple radiocarbon calibration (Stuiver & Reimer, 1993).

Nosterfield, the Flasks, Core 69 (Table 6; Fig. 6)

The four samples from core 69 (see Chapter 3.2.3) were dated to provide a chronology for sediment accumulation at the site and to allow correlation between this core and other dated sequences at Nosterfield. The results show that organic detrital sediment accumulation above an inorganic shell-rich clay started at 10,990–10,880 cal. BC (OxA-12997; 10,920±45 BP), with the appearence of an increasingly clayey component within the sediment sequence occurring at 10,780–10,280 cal. BC (OxA-12972; 10,510±55 BP). The clay represents the increasingly cold climatic conditions of the Loch Lomond Stadial. Sample OxA-12932 (83–85 cm) provides a date (9760–9310 cal. BC) for the main rise in *Betula* frequencies recorded in the pollen record and thus the replacement of the more open habitat herbaceous plant cover associated with Lateglacial assemblages. The top of the undisturbed peat in Core 69 dates to 7960–7590 cal. BC (OxA-12960).

Table 6: Details of radiocarbon dates from Nosterfield, the Flasks 69

Laboratory code	Sample depth	Material	δ13C (‰)	Radiocarbon age BP	Calibrated date range(95% confidence)
OxA-12960	49–50cm	Indeterminate bark	-27.5	8725±45	7960–7590 cal BC
OxA-12932	83–85cm	Plant macrofossils: *Schoenoplectus lacustris* nutlets, *Menyanthes trifoliata* seed, *Betula* sp. fruit	-26.5	9990±45	9760–9310 cal BC
OxA-12972	153–54cm	Plant macrofossils: 3 *Carex* sp. trigonous nutlets, Salicaceae? root, Ericaceae stem	-27.5	10,510±55	10780–10280 cal BC
OxA-12997	163–64cm	Plant macrofossils: 3 *Carex* sp. trigonous nutlets, cf. Salicaceae wood, ?monocot fragment	-29.2	10,920±45	10990–10880 cal BC

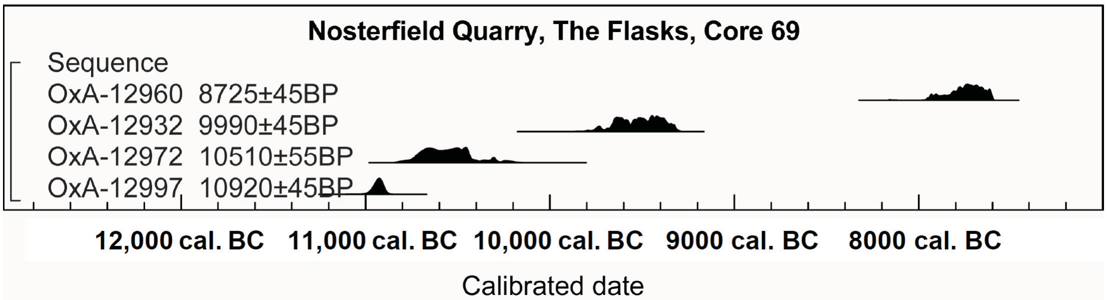

Figure 6: Probability distributions of dates from Nosterfield, Core 69. Each distribution represents the relative probability that an event occurred at a particular time. These distributions are the result of simple radiocarbon calibration (Stuiver & Reimer, 1993).

Newby Wiske (Table 7; Fig. 7)

Eight samples were submitted from the site at Newby Wiske (Chapter 3.3) to provide a chronological framework for the Lateglacial and Holocene peat and marl deposits and the major vegetation changes recorded within the pollen record. The results (Fig. 7) show poor agreement between the radiocarbon results and their stratigraphical positions; in particular OxA-13112 seems to be far too young. This sample comprised *Betula* fruits and bud scales and was intended to provide a date for the pollen zone boundary defined by the main fall in *Betula* and the early Holocene rise in *Corylus* to its rational limit. This event is usually dated to around 8250 cal. BC (*c*. 9000 BP). Given the integrity of the pollen record, containing the complete expected sequence of pollen zone changes throughout the early Holocene, movement of material down profile seems unlikely. No plausible explanation, other than some form of contamination, can be offered; why such contamination would not have shown itself in the fossil records is puzzling.

Table 7: Details of radiocarbon dates from Newby Wiske

Laboratory code	Sample depth	Material	δ13C (‰)	Radiocarbon age BP	Calibrated date range (95% confidence)
GrA-25031	1–2cm	Indeterminate bark	-26.6	4315±40	3030–2880 cal. BC
OxA-13321	54–56cm	Wood: *Alnus glutinosa*	-27.4	4921±33	3780–3640 cal. BC
OxA-13322	61–62cm	Wood: *Alnus glutinosa*	-26.5	5241±32	4230–3970 cal. BC
GrA-25028	191–92cm	Wood: *Alnus* wood	-26.9	8040±50	7090–6770 cal. BC
OxA-13226	204–05cm	Plant macrofossils: *Eupatorium cannabinum* achenes, *Betula* sp. fruits, *Carex* sp. nutlet, *Nymphaea alba*, *Sparganium* subgen. *Xanthosparganium* nutlets	-25.8	8265±45	7480–7080 cal. BC
OxA-13107	214–15cm	Plant macrofossils: fruits and nutlets of *Eupatorium*, *Mentha*, *Betula*, *Sparganium* subgen. *Xanthosparganium*, *Carex*; bark cylinder	-27.8	8660±55	7800–7580 cal. BC
OxA-13112	341–43cm	Plant macrofossils: *Betula* fruits and bud scales	-28.0	6710±50	5720–5540 cal. BC
GrA-25030	355–56cm	Plant macrofossils: monocot stems	-22.5	11,280±60	11,330–11,120 cal. BC

The pollen evidence also suggests that the basal measurement from the site (GrA-25030) is incorrect, this time the result being too old for the deposit from which it was obtained. The sample should provide an age as close as possible to the main early Holocene rise in *Betula* pollen: by analogy with other dated sequences a little after *c*. 9500 cal. BC (*c*. 10,000 BP). The calibrated result 11,330–11,120 cal. BC, however, is clearly too old and might suggest that the base of the sequence contained redeposited material, perhaps from an erosional episode. The remaining six results show good agreement with their stratigraphical positions and with the expected ages of vegetational events in the pollen record.

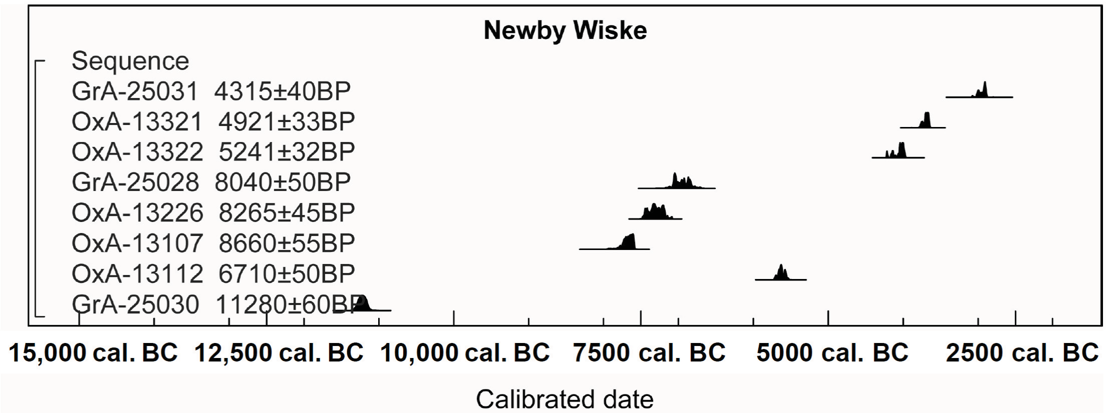

Figure 7: Probability distributions of dates from Newby Wiske. Each distribution represents the relative probability that an event occurred at a particular time. These distributions are the result of simple radiocarbon calibration (Stuiver & Reimer, 1993).

Sharow Mires (Table 8; Fig. 8)

A core comprising almost 11 m of variously organic sediments was recovered from Sharow Mires, a lowland area that marks an abandoned channel of the River Ure

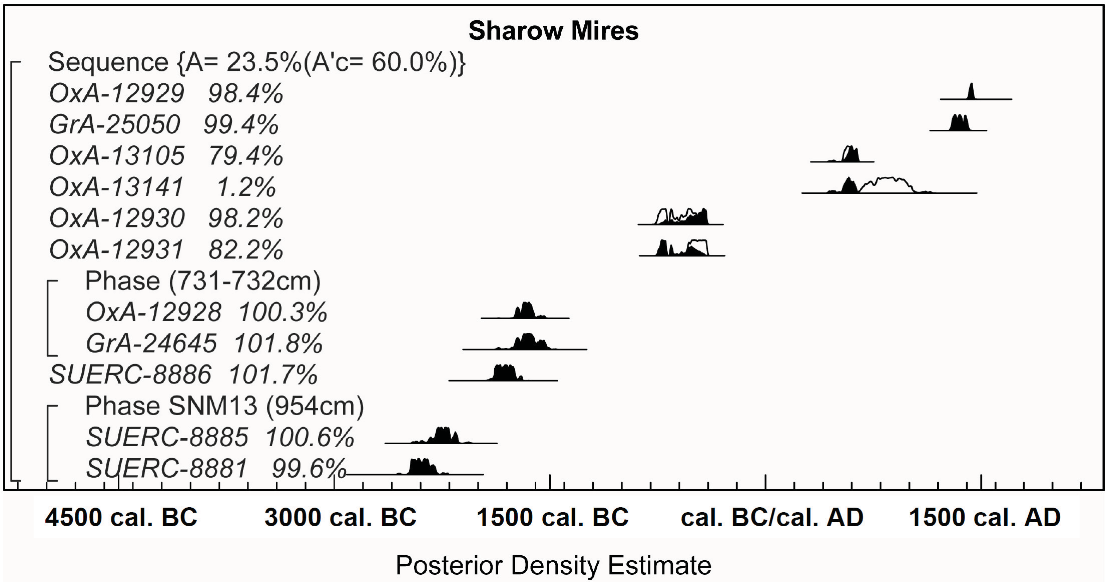

Figure 8a: Probability distributions of dates from Sharow Mires. Each distribution represents the relative probability that an event occurs at a particular time. For each of the radiocarbon dates two distributions have been plotted, one in outline, which is the result of simple radiocarbon calibration, and a solid one, which is based on the chronological model used. The large square brackets down the left hand side along with the OxCal keywords define the model exactly.

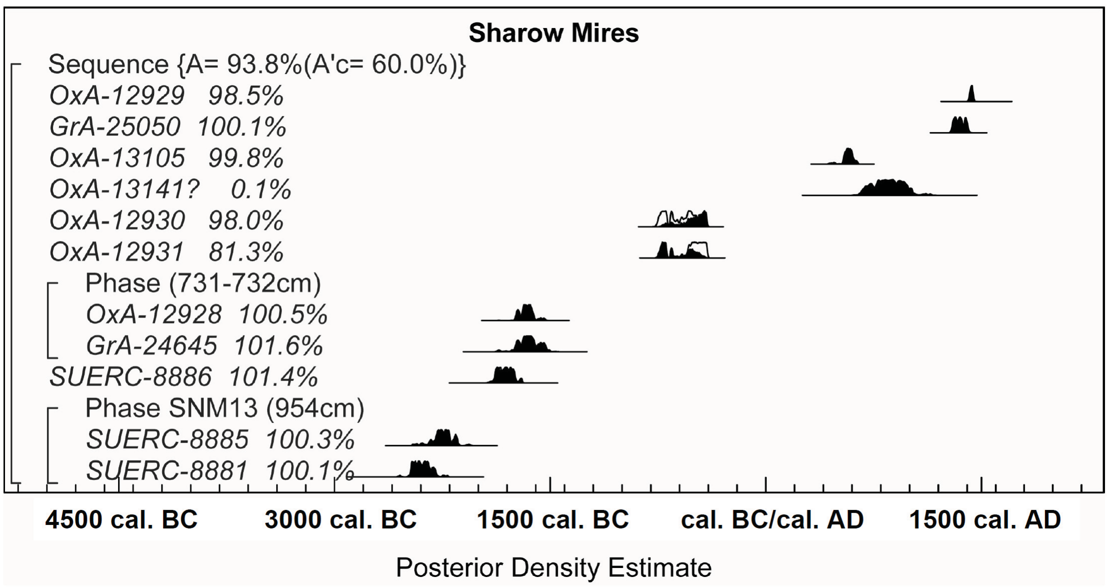

Figure 8b: Probability distributions of dates from Sharow Mires. Each distribution represents the relative probability that an event occurs at a particular time. For each of the radiocarbon dates two distributions have been plotted, one in outline, which is the result of simple radiocarbon calibration, and a solid one, which is based on the chronological model used. A question mark (*?*) indicates that the result has been excluded from the model The large square brackets down the left hand side along with the OxCal keywords define the model exactly.

Table 8: Details of radiocarbon dates from Sharow Mires

Laboratory code	Sample depth	Material	$\delta^{13}C$ (‰)	Radiocarbon age BP	Weighted mean	Calibrated date range (95% confidence)	*Posterior Density Estimate (95% probability)*
OxA-12929	173–174cm	Plant macrofossils: 2 *Rumex* sp. nutlets, 5.5 *Carex* sp. trigonous nutlets, 1 *Betula* sp. Fruit	-27.2	482±27		cal. AD 1410–1450	*cal. AD 1410–1450*
GrA-25050	253–254cm	Plant macrofossils: monocot stems	-26.7	605±35		cal. AD 1280–1420	*cal. AD 1290–1410*
OxA-13105	476–477cm	Plant macrofossils: *Rumex* sp. nutlet, 2 monocot stems	-28.4	1494±28		cal. AD 530–640	*cal. AD 460–480 (2%) or 530–650 (93%)*
OxA-13141	479–482cm	Plant macrofossils: *Menyanthes trifoliata*, monocot stem, cf. Salicaceae stem	-27.1	1170±100		cal. AD 650–1030	-
OxA-12930	530–531cm	Wood: *Alnus glutinosa* stem	-29.0	2450±31		770–400 cal. BC	*720–400 cal. BC*
OxA-12931	616cm	Wood: *Alnus* large chunk	-27.2	2426±30		750–400 cal. BC	*760–630 (51%) or 600–420 (44%) cal. BC*
GrA-24645	731–732cm	Plant macrofossil: cf. Salicaceae	-30.4	3360±50	T'=0.0; ν=1; T'(5%)=3.8	1760–1510 cal. BC	*1750–1520 cal. BC*
OxA-12928	731–732cm	Plant macrofossils: 10 *Carex* sp. trigonous nutlets, 1 *Lycopus europaeus*, 1 *Rumex* sp., 2 *Alisma* spp.	-24.4	3371±31		1750–1540 cal. BC	*1750–1600 (91%) or 1580–1530 (4% cal. BC*
SUERC-8886	SM 893cm	Wood: *Alnus*	-29.9	3485±35		1900–1690 cal. BC	*1900–1730 (94%) or 1710–1690 (1%) cal. BC*
SUERC-8881	SM 954cm	Hazelnut fragment	-26.4	3905±35	T'=4.1; ν=1; T'(5%)=3.8	2480–2280 cal. BC	*2480–2280 cal. BC*
SUERC-8885	SM 954cm	4 twigs	-30.5	3805±35		2400–2130 cal. BC	*2410–2380 (2%) or 2350–2130 (93%) cal. BC*

(Chapter 2; Chapter 3.5). The eleven dated samples provide a chronological framework for establishing human impact on the landscape and vegetation history.

The replicate samples from 954 cm are not statistically consistent (T'=4.1; ν=1; T'(5%)=3.8; Ward & Wilson, 1978), although they only just fail a chi-squared test. However, the two samples from 731–732 cm are statistically consistent (T'=0.0; ν=1; T'(5%)=3.8; Ward & Wilson, 1978) and could thus represent material of the same age.

The model shown in Figure 8a shows poor overall agreement between the radiocarbon results and stratigraphy ($A_{overall}$=23.5%), with sample OxA-13141 (479–482 cm) having a very low individual index of agreement (A=1.2%). If this sample is excluded from the analysis (Fig. 8b), the model shows good agreement ($A_{overall}$=93.8%). Sample OxA-13141 would therefore appear to have produced a result too young for its stratigraphical position. The remaining results provide a detailed chronological sequence from the early Bronze age to the Medieval period.

Ripon North (Table 9; Fig. 9)

Two samples from the Hanson's quarry at Ripon (Ripon North: Chapter 3.6) were dated. A fully round piece of alder wood (GU-5998), extracted from the upper part of the gravel sequence, provides a date (2560–2200 cal. BC) for the end of gravel aggradation and a *terminus post quem* for the start of fine-grained sediment deposition above the gravels. GrA-25377, from the organic fine-grained sediment, was dated 510–230 cal. BC.

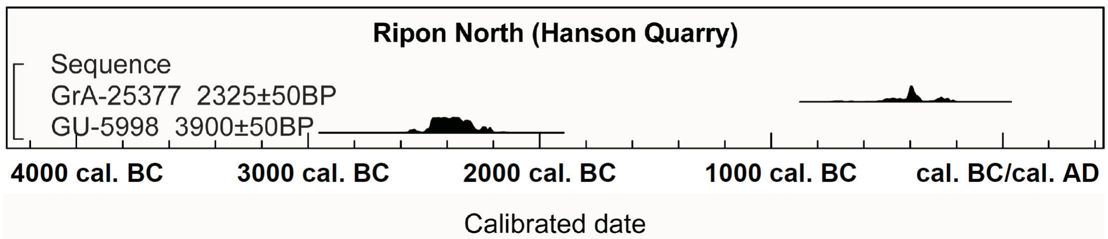

Figure 9: Probability distributions of dates from Ripon North (Hanson's Quarry). Each distribution represents the relative probability that an event occurred at a particular time. These distributions are the result of simple radiocarbon calibration (Stuiver & Reimer, 1993).

Table 9: Details of radiocarbon dates from Ripon North (Hanson's quarry)

Laboratory code	Sample depth	Material	δ13C (‰)	Radiocarbon age BP	Calibrated date range (95% confidence)
GU-5998	RH wood	Wood: *Alnus glutinosa* wide roundwood	-25.9	3900±50	2560–2200 cal. BC
GrA-25377	69–70cm	Plant macrofossils: *Polygonum aviculare*, *Polygonum* spp., Chenopodiaceae, *Pteridium* spp.	-28.1	2325±50	510–230 cal. BC

Ripon South (Table 10; Fig. 10)

The five samples submitted from Brown & Potter's quarry at Ripon South (Chapter 3.7) were selected with the intention of:

- providing a minimum age for the incision of the Ure to its present position (samples from basal monolith 2M);
- establishing a chronology for the start and end of organic sedimentary infill of an upper channel (possible oxbow);
- establishing the age of agricultural expansion as shown by an increase in cereal pollen.

The two samples from the basal organic deposit (monolith 2M) at the site (OxA-12748; 3896±31 & OxA-12636; 4011±40) are not statistically consistent (T'=5.2; ν=1; T'(5%)=3.8; Ward & Wilson, 1978) and are therefore of different ages. However, given that the results only just fail a chi-squared test and come from a deposit that might be expected to have formed over a period of time, rather than in a single event, there is no reason to suspect that they do not provide accurate age estimates for the deposit. OxA-12748 (2480–2280 cal. BC) therefore provides a basal age for the terrace deposits at this site. OxA-12251 (725±25 BP) provides a date (cal. AD 1220–1290) for the start of the first coarsening upwards sequence within the upper channel-fill sequence and OxA-12252 (627±27 BP) for the start (cal. AD 1280–1410) of the third such coarsening upwards cycle, coinciding with an increase in cereal-type pollen. OxA-12553 (504±26 BP) gives an age (cal. AD 1400–1450) for the end of peat accumulation and the start of the fourth coarsening upwards cycle.

In addition to the five samples submitted as part of the ALSF project, a bulk sample from a peat bed exposed during an earlier phase of quarrying by Brown and Potter was dated (Beta-116457; 9710±60 BP) by Howard *et al*. (2000). This was located within an older, higher terrace (see Chapter 2.6.4 & Chapter 3.7), so the date indicates that incision by the River Ure formed that terrace sometime after 9290–8860 cal. BC.

Table 10: Details of radiocarbon dates from Ripon South (Brown & Potter's quarry)

Laboratory code	Sample depth	Material	δ13C (‰)	Radiocarbon age BP	Weighted mean	Calibrated date range (95% confidence)
OxA-12553	15cm	Plant macrofossil: *Rumex* sp.	-26.9	504±26		cal. AD 1400–1450
OxA-12552	65cm	Plant macrofossil: *Rumex* sp.	-28.2	627±27		cal. AD 1280–1410
OxA-12551	125cm	Plant macrofossils: *Rumex* sp., Chenopodiaceae sp., Caryophyllaceae sp., *Sonchus* sp.	-28.5	752±25		cal. AD 1220–1290
OxA-12748	208cm	Wood: *Corylus* fragments	-31.2	3896±31	T'=5.2; ν=1; T'(5%)=3.8	2480–2280 cal. BC
OxA-12636	208cm	Plant macrofossil: Cyperaceae spp.	-26.1	4011±40		2630–2460 cal. BC
Beta-116457	Howard *et al.* (2000)	Peat	-	9710±60		9290–8860 cal. BC

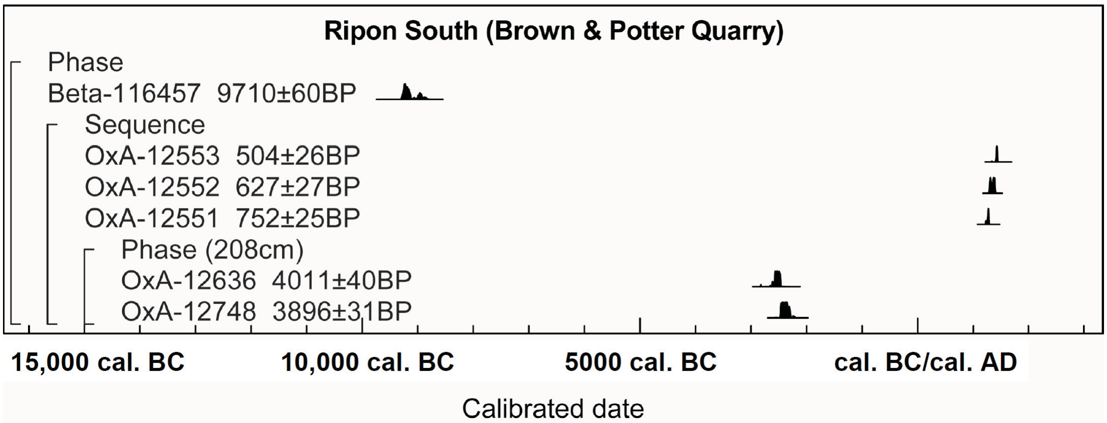

Figure 10: Probability distributions of dates from Ripon South (Brown & Potter Quarry). Each distribution represents the relative probability that an event occurred at a particular time. These distributions are the result of simple radiocarbon calibration (Stuiver & Reimer, 1993).

Snape Mires, Ings Plantation, core 12A (Table 11; Fig. 11)

Core 12A represents the deepest peat recorded in a transect of cores across the northern part of the Snape Mires glacio-lacustrine basin (Chapter 3.8). The stratigraphical record shows approximately 50 cm of peat overlying shell marl, underneath which *limus* is recorded before coring reached stiff blue clay and gravel. The radiocarbon results show that the base of the core dates to the early Holocene 9870–9400 cal. BC; (SUERC-8574), and the maximum *Betula* frequencies in the pollen record date from 9190–8720 cal. BC (SUERC-8573). The two measurements from SNM8 (IL12 79–81 cm) are statistically consistent (T'=1.1; ν=1; T'(5%)=3.8; Ward & Wilson, 1978) and date the increase in *Corylus* in the pollen record to the mid-9th Millennium cal. BC

Table 11: Details of radiocarbon dates from Snape Mires, Ings Plantation core 12A

Laboratory Code	Sample depth	Material	δ13C (‰)	Radiocarbon Age (BP)	Weighted mean	Calibrated Date (95% confidence)
SUERC-8568	79–81cm	Plant macrofossils: *Betula* fruits, Cyperaceae nutlets & *Menyanthes* seeds	-28.4	9270±40	T'=1.1; ν=1; T'(5%)=3.8	8710–8470 cal. BC
SUERC-8569	79–81cm	Twigs	-29.6	9330±40		8630–8330 cal. BC
SUERC-8573	125cm	Plant macrofossils: Cyperaceae nutlets, *Betula* fruits & bract	-28.4	9545±55		9190–8720 cal. BC
SUERC-8574	142cm	Plant macrofossils: *Menyanthes* seeds & Cyperaceae nutlets	-26.5	10,060±40		9870–9400 cal. BC

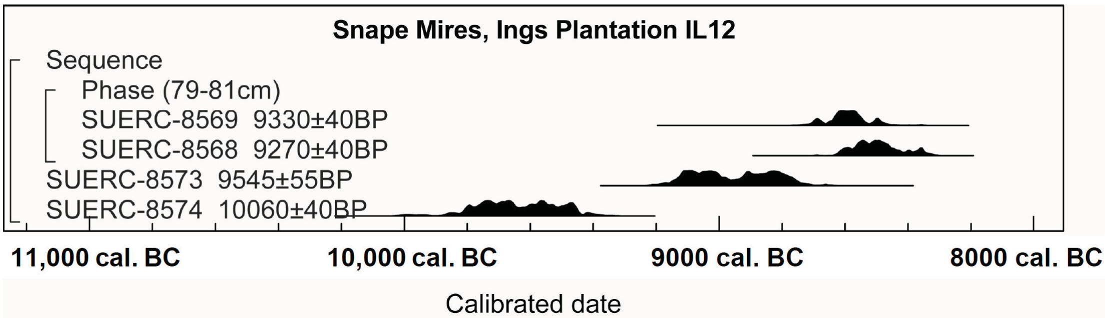

Figure 11: Probability distributions of dates from Snape Mires, Ings Plantation, core 12A (IL12). Each distribution represents the relative probability that an event occurred at a particular time. These distributions are the result of simple radiocarbon calibration (Stuiver & Reimer, 1993).

Snape Mires, Mill House 1 (Table 12; Fig. 12)

The four measurements from the Snape Mill (Mill House 1) tufa site (see Chapter 3.8.3) show that sedimentation here was taking place from the Lateglacial (12,650–12,110 cal. BC; SUERC-8567) to the early Holocene (9190–8770 cal. BC; SUERC-8879).

Table 12: Details of radiocarbon dates from Snape Mires, Mill House 1

Laboratory Code	Sample depth	Material	δ13C (‰)	Radiocarbon Age (BP)	Calibrated Date (95% confidence)
SUERC-8879	131cm	Plant macrofossils: *Betula* fruits & bracts, *Carex* nutlets	-24.5	9580±40	9190–8770 cal. BC
SUERC-8880	145cm	Charred twigs	-25.1	10,040±45	9820–9360 cal. BC
SUERC-8566	248cm	Plant macrofossils: *Carex* & *Betula* fruits, nutlets & twigs	-28.1	11,310±45	11,330–11,150 cal. BC
SUERC-8567	439cm	Plant macrofossils: *Eleocharis* nutlets & unidentified twigs	-27.1	12,330±45	12,650–12,110 cal. BC

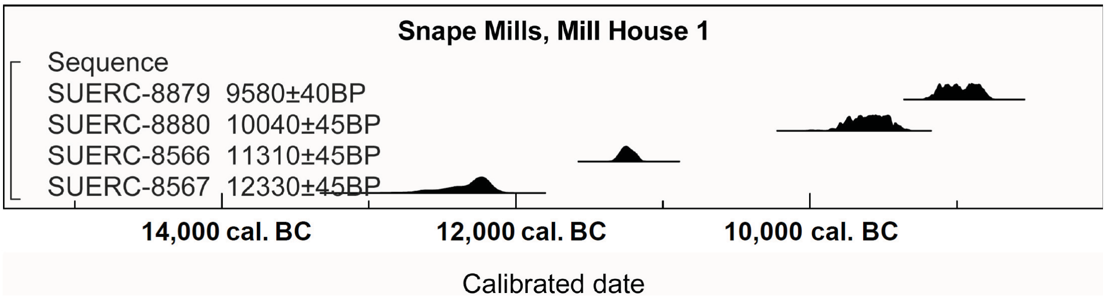

Figure 12: Probability distributions of dates from Snape Mires, Mill House 1. Each distribution represents the relative probability that an event occurred at a particular time. These distributions are the result of simple radiocarbon calibration (Stuiver & Reimer, 1993).

Snape Mires, the Gallop (Table 13; Fig. 13)

The Gallop lies at the centre of the Snape Mires basin, where there is a thin peat, overlying shell marl, *limus*, and glacio-lacustrine clay (Chapter 3.8.4). Replicate samples were submitted from the base of the peat where it overlies the shelly marl. The two measurements are statistically consistent (T'=1.1; ν=1; T'(5%)=3.8; Ward & Wilson, 1978) and could therefore be of the same age. The results show that peat started to accumulate at the Gallop in the late 10th to early 9th Millennium cal. BC.

Table 13: Details of radiocarbon dates from Snape Mires, the Gallop

Laboratory Code	Sample depth	Material	δ13C (‰)	Radiocarbon Age (BP)	Weighted mean	Calibrated Date (95% confidence)
SUERC-8887	77cm	Plant macrofossils: *Carex & Lycopus* nutlets *and* *Menyanthes* seeds	-25.0	9515±40	T'=1.1; ν=1; T'(5%)=3.8	9130–8720 cal. BC
SUERC-8888	77cm	Plant macrofossils: *Carex & Lycopus* nutlets *and* *Menyanthes* seeds	-25.9	9475±40		9190–8760 cal. BC

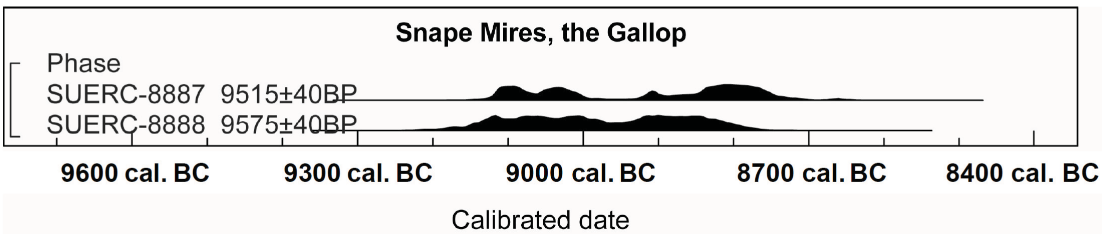

Figure 13: Probability distributions of dates from Snape Mires, the Gallop. Each distribution represents the relative probability that an event occurred at a particular time. These distributions are the result of simple radiocarbon calibration (Stuiver & Reimer, 1993).

Langland's Farm (Table 14; Fig. 14)

A single sample was submitted from Langland's Farm (Chapter 3.9.1) to provide an age for the start of sediment accumulation and the end of peat accumulation at the site. The sample (GrA-24660), from the base of the organic-rich silts close to the top of the peat, was dated 4460–4260 cal. BC.

Table 14: Details of radiocarbon dates from Langland's Farm

Laboratory code	Sample depth	Material	δ13C (‰)	Radiocarbon age BP	Calibrated date range (95% confidence)
GrA-24660	69–70cm	Wood: cf. *Alnus glutinosa*	-28.8	5520±50	4460–4260 cal. BC

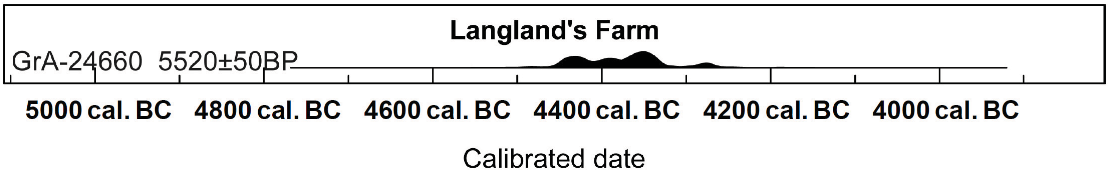

Figure 14: Probability distributions of dates from Langland's Farm. Each distribution represents the relative probability that an event occurred at a particular time. These distributions are the result of simple radiocarbon calibration (Stuiver & Reimer, 1993).

Thornton's Plantation (Table 15; Fig. 15)

Replicate samples from the top of the peat bed at Thornton's Plantation (Chapter 3.9.2) were submitted to provide a date for the end of peat accumulation and a *terminus post quem* for the onset of river alluviation. The two measurements (GrA-24656; 9060±60 BP and GrA-25290 8850±50 BP) are statistically inconsistent (T'=7.3; ν=1; T'(5%)=3.8; Ward & Wilson, 1978) implying that this horizon contains material of different ages. The youngest result GrA-25290 (8230–7740 cal. BC) can be used, however, to provide the best estimate for the change from pure peat deposition to organic sedimentation at the site.

Table 15: Details of radiocarbon dates from Thornton's Plantation

Laboratory code	Sample depth	Material	δ13C (‰)	Radiocarbon age BP	Weighted mean	Calibrated date range (95% confidence)
GrA-24656	74–75cm	Plant macrofossils: herbaceous plant remains	-28.2	9060±60	T'=7.3; ν=1; T'(5%)=3.8	8340–8220 cal. BC
GrA-25290	74–75cm	Wood: *Corylus*/*Alnus* twig and unidentified bark	-29.3	8850±50		8230–7740 cal. BC

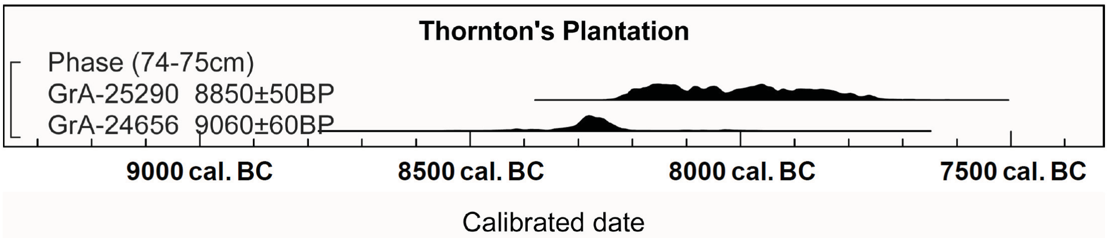

Figure 15: Probability distributions of dates from Thornton's Plantation. Each distribution represents the relative probability that an event occurred at a particular time. These distributions are the result of simple radiocarbon calibration (Stuiver & Reimer, 1993).

Conclusions

The radiocarbon results have generated the first robust chronological framework for understanding the vegetation and landscape history of this part of lowland northern Britain. The results have also provided important new information on the timing and nature of river dynamics, climate changes and human impact on vegetation and landscape stability. A fundamental part of the success of the dating programme has been the use of a rigorous methodology for identifying potential samples for radiocarbon analysis. Although initially time consuming, e.g. in retrieving and identifying plant macrofossils, etc, it has paid dividends and highlights the importance of resolving 'taphonomic problems', if precise chronologies are to be constructed.

References

Aerts-Bijma, A.T., Meijer, H.A.J. & van der Plicht, J. (1997) AMS sample handling in Groningen. *Nuclear Instruments and Methods in Physics Research B*, **123**, 221–225.

Aerts-Bijma, A.T., van der Plicht, J. & Meijer, H.A.J. (2001) Automatic AMS sample combustion and CO_2 collection. *Radiocarbon*, **43**, 293–298.

Birks, H.J.B. & Birks, H.H. (1980) *Quaternary Palaeoecology*. Edward Arnold, London.

Blockley, S.P.E., Lowe, J.J., Walker, M.J.C., Asioli, A., Trincardi, F., Coope, G.R., Donahue, R.E. & Pollard, A.M. (2004) Bayesian analysis of radiocarbon chronologies: examples from the European Late-glacial. *Journal of Quaternary Science*, **19**, 159–175.

Bowman, S. (1990) *Interpreting the Past: Radiocarbon Dating*. British Museum Publications, London.

Bronk Ramsey, C. (1995) Radiocarbon Calibration and Analysis of Stratigraphy: The OxCal Program. *Radiocarbon*, **37**, 425–430.

Bronk Ramsey, C. (1998) Probability and dating. *Radiocarbon*, **40**, 461–474.

Bronk Ramsey, C. (2001) Development of the radiocarbon dating program Oxcal. *Radiocarbon*, **43**, 355–363.

Bronk Ramsey, C. & Hedges, R.E.M. (1997) A gas ion source for radiocarbon dating. *Nuclear Instruments and Methods in Physics Research B* **29**, 45–49.

Bronk Ramsey, C., Higham, T. & Leach, P. (2004) Towards high precision AMS: progress and limitations. *Radiocarbon*, **46**, 17–24.

Bronk Ramsey, C., Pettitt, P.B., Hedges, R.E.M., Hodgins, G.W.L. & Owen, D.C. (2000) Radiocarbon dates from the Oxford AMS system: Archaeometry datelist 30. *Archaeometry*, **42**, 259–279.

Buck, C.E., Cavanagh, W.G. & Litton, C.D. (1996) *Bayesian Approach to Interpreting Archaeological Data*. Wiley, Chichester.

Gelfand A.E. & Smith, A.F.M. (1990) Sampling approaches to calculating marginal densities. *Journal of the American Statistical Society*, **85**, 398–409.

Gilks, W.R., Richardson, S. & Spiegelhalter, D.J. (1996) *Markov Chain Monte Carlo in Practice*. Chapman & Hall, London.

Howard, A.J., Keen, D.H., Mighall, T.M., Field, M.H., Coope, G.R., Griffiths, H.I. & Macklin, M.G. (2000) Early Holocene environments of the River Ure near Ripon, North Yorkshire, UK. *Proceedings of the Yorkshire Geological Society*, **53**, 31–42.

Lowe, J.J. & Walker, M.J.C. (1997) *Reconstructing Quaternary Environments*. Addison Wesley Longman, London.

Lowe, J.J. & Walker, M.J.C. (2000) Radiocarbon dating the last glacial–interglacial transition (^{14}C ka BP) in terrestrial and marine records: the need for new quality assurance protocols. *Radiocarbon*, **42**, 53–68.

Mook, W.G. (1986). Business meeting: recommendations/resolutions adopted by the twelfth international radiocarbon conference. *Radiocarbon,* **28**, 799.

Noakes, J.E., Kim, S.M. & Stipp, J.J. (1965) Chemical and counting advances in Liquid Scintillation Age dating. In: *Proceedings of the Sixth International Conference on Radiocarbon and Tritium Dating* (eds E.A. Olsson & R.M. Chatters), pp. 68–92, Washington State University, Pullman WA. U.S. Atomic Energy Commission, CONF-650652.

Scott, E.M. (2003) The third international radiocarbon intercomparison (TIRI) and the fourth international radiocarbon intercomparison (FIRI) 1990–2002: results, analyses and conclusions. *Radiocarbon*, **45**, 135–408.

Shore, J.S., Bartley, D.D. & Harkness, D.D. (1995) Problems encountered with the ^{14}C dating of peat. *Quaternary Science Reviews*, **14**, 373–383.

Slota, J.P.J., Jull, A.J.T., Linick, T.W. & Toolin, L.J. (1987) Preparation of small samples for ^{14}C accelerator targets by catalytic reduction of CO. *Radiocarbon*, **29**, 303–306.

Smith, A.G. & Pilcher, J.R. (1973) Radiocarbon dates and vegetational history of the British Isles. *New Phytologist*, **72**, 903–914.

Stenhouse, M.J. & Baxter, M.S. (1983) ^{14}C dating reproducibility: evidence from routine dating of archaeological samples. *PACT*, **8**, 147–161.

Stuiver, M. & Kra, R.S. (1986) Editorial comment. *Radiocarbon*, **28 (2B)**, ii.

Stuiver, M. & Polach, H.A. (1977) Reporting of ^{14}C data. *Radiocarbon*, **19**, 355–363.

Stuiver, M. & Reimer, P.J. (1986) A computer program for radiocarbon age calculation. *Radiocarbon*, **28**, 1022-1030.

Stuiver, M. & Reimer, P.J. (1993) Extended ^{14}C data base and revised CALIB 3.0 ^{14}C age calibration program. *Radiocarbon*, **35**, 215–230.

Tipping, R.M. (2000) Nosterfield, North Yorkshire. Report on the completion of ^{14}C dating for sediments from F44, F45, F36 and FIND 14: recommendations and proposals for further work. Department of Enviromental Science, University of Stirling. Mike Griffiths & Associates.

van der Plicht, J., Wijma, S., Aerts, A. T., Pertuisot, M.H. & Meijer, H.A.J. (2000) Status report: the Groningen AMS facility. *Nuclear Instruments and Methods in Physics Research B*, **172**, 58–65.

Walker, M.J.C., Bryant,C., Coope, G.R., Harkness, D.D., Lowe, J.J. & Scott, E.M. (2001) Towards a radiocarbon chronology of the Late-Glacial: sample selection strategies. *Radiocarbon*, **43**, 1007–1021.

Ward, G.K. & Wilson, S.R. (1978) Procedures for comparing and combining radiocarbon age determinations: a critique. *Archaeometry*, **20**, 19–31.

Xu, S., Anderson, R., Bryant, C., Cook, G.T., Dougans, A., Freeman, S., Naysmith, P., Schnabel, C. & Scott, E.M. (2004) Capabilities of the new SUERC 5MV AMS facility for ^{14}C dating. *Radiocarbon*, **46**, 59–64.